

# Complexation Thermodynamics of Cyclodextrins in the Framework of a Molecular Size-Based Model for Nonassociative Organic Liquids That Includes a Modified Hydration-Shell Hydrogen-Bond Model for Water

Peter Buchwald<sup>†</sup>

IVAX Research, Inc., 4400 Biscayne Boulevard, Miami, Florida 33137

Received: March 1, 2002

The complexation thermodynamics of a large number of guest molecules with natural  $\alpha$ -,  $\beta$ -, and  $\gamma$ -cyclodextrins (CD) can be well-described within the framework of a recently introduced, unified, molecular size-based model for nonassociative liquids that also includes a modified hydration-shell hydrogen-bond model for water (Buchwald, P.; Bodor, N. *J. Am. Chem. Soc.* **2000**, *122*, 10671). With increasing guest size, 1:1 complex stability, as measured by  $\ln K$  or  $\Delta G^\circ$ , tends to increase linearly up to a size limit characteristic for each CD. For  $\alpha$ - and  $\beta$ -CD, the corresponding slopes and intercepts are in excellent agreement with those predicted by the model. For larger guest structures, values level off and are scattered around an average value depending on shape, goodness of fit, and possibly lipophilicity and some specific effects (e.g., such as those caused by presence of phenol functionality). It is an important achievement in the description of interactions in liquids that the very same interaction constants derived from boiling point and enthalpy of vaporization data can describe partition, and now complex stability data as well. Furthermore, for most molecules, heat capacity changes associated with complex formation are also in excellent agreement with those derived from the model based on hydrogen bonding changes in the hydration shell.

## Introduction

The purpose of the present paper is to show that a recently introduced unified, molecular size-based model for nonassociative organic liquids and water<sup>1–3</sup> can also describe cyclodextrin (CD) host–guest complexation. This is not surprising, because the model gives very good quantitative description for nonassociative liquids and can also be extended to describe water and partition/solubility in water by combining it with a modified hydration-shell hydrogen-bond model.<sup>2,3</sup>

Cyclodextrins are torus-shaped oligosaccharides that contain various numbers of  $\alpha$ -1,4-linked glucose units (6, 7, and 8 for  $\alpha$ -,  $\beta$ -, and  $\gamma$ -CD, respectively). The number of units determines the size of the inside cavity that tends to have a truncated cone shape with the secondary hydroxyl groups along its wider edge and the primary hydroxyl groups along its narrower edge (Figure 1). Various compounds can include within this cavity to form stable complexes.<sup>4–7</sup> Natural CDs and their derivatives are now widely used in pharmaceutical, cosmetic, or food industries to enhance solubility, to stabilize hydrolytically or otherwise unstable compounds, to enhance bioavailability, to transform liquids into powders, to improve smell or taste characteristics by prevention of evaporation, to reduce possible stomach injuries, to inhibit hemolysis, or other purposes. Characterizing the stability of CD complexes was of particular interest for us because of their many applications in what is designated now as retrometabolic drug design.<sup>8–11</sup>

Formation of CD inclusion complexes is known to involve mainly nonspecific, weak interactions and no covalent bonding. Therefore, the transfer of organic guest molecules from the aqueous solution into the cyclodextrin cavity is in many aspects

very similar to the transfer (partition) that takes place between an aqueous and a somewhat hydrophobic organic phase.<sup>7</sup> As our model described the latter partition very well,<sup>1,3</sup> one should be able to extend it to describe inclusion complexation with cyclodextrins as well.

There have been a number of more or less successful attempts to describe or predict the free energies of cyclodextrin complex formation.<sup>12</sup> For example, more recent attempts were made by simply summarizing statistical properties,<sup>13,14</sup> by proceeding from a phenomenological description,<sup>15</sup> by using overall molecular descriptors,<sup>16,17</sup> by using a group-contribution method,<sup>18</sup> or even by applying a genetic algorithm approach.<sup>19,20</sup> Contrary to these works, the main focus of the present paper is not as much to accurately predict binding constants, but to place the physicochemistry of complex formation into a general descriptive framework developed for organic liquids.

## Methods/Experimental Data

Experimental thermodynamic data, such as log complex stability constants ( $\log K$ ), standard free energies ( $\Delta G^\circ$ ), and heat capacities ( $\Delta C_p^0$ ) for 1:1 inclusion complexation of a large variety of guests with natural  $\alpha$ -,  $\beta$ -, and  $\gamma$ -CDs were collected from the literature. A considerable amount of such data was compiled by Rekharsky and Inoue in their review article on complexation thermodynamics.<sup>7</sup> Additional standard free energy data were collected from recent publications by Castronuovo and co-workers,<sup>21</sup> Klein and co-workers,<sup>16,17</sup> and T. Suzuki.<sup>18</sup> For compounds with more experimental data available, average values were used. Data for amines were also included even if the correction for protonation was not done rigorously in some cases. These values may be somewhat more scattered, but they seemed sufficiently consistent. Experimental octanol–water partition data are from the compilation of Hansch and co-

<sup>†</sup> Phone: (305) 575-4021. Fax: (305) 575-6027. E-mail: Peter\_Buchwald@ivax.com.

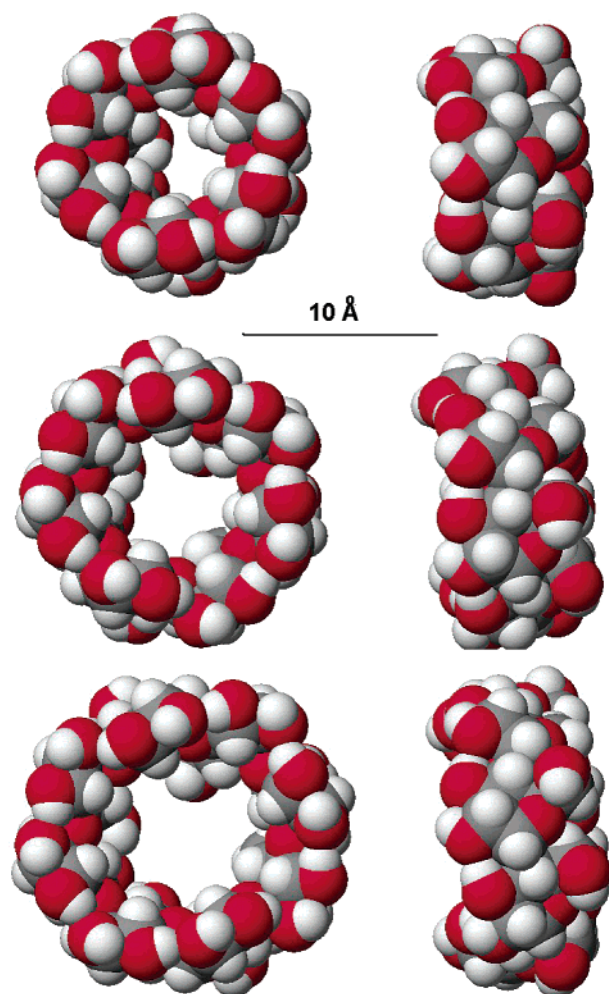


**Figure 1.** CPK structures showing fully AM1-optimized geometries for natural  $\alpha$ -,  $\beta$ -, and  $\gamma$ -cyclodextrins containing  $\alpha$ -1,4-linked 6, 7, and 8 glucose units, respectively. These structures tend to have a truncated cone shape with the secondary hydroxyls along the wider edge (front and left side, respectively) and the primary hydroxyls along the narrower edge.

workers;<sup>22</sup> calculated values were obtained using the QLogP program.<sup>2,23,24</sup> Detailed data are included in the Supporting Information. Three-dimensional molecular structures were built and the corresponding molecular volumes, used here as size descriptor, were calculated using computer models and softwares as described in our previous publications.<sup>1,3</sup> Cyclodextrin structures used for illustration were fully geometry-optimized using AM1 semiempirical quantum chemical calculations<sup>25</sup> in CAChe 5.0 (Fujitsu, Ltd., Chiba, Japan). Statistical analyses and curve fitting were performed using a standard spreadsheet program (Microsoft Excel 97).

## Results and Discussion

**Complex Stability: Size Effects.** As generally done for properties included in the model, the equation describing complex stability constants and/or corresponding standard free energies is obtained starting from the general form of the chemical potential  $\mu_i^{\text{sol},j}$  of solute  $i$  in solvent  $j$ :<sup>1-3</sup>

$$\mu_i^{\text{sol},j} = kT \ln \left( \frac{\rho_i}{f} \Lambda_i^3 \right) - \left( w_{ij} + \frac{kT}{v_j} \right) v_i - w_0 + kT \quad (1)$$

Here  $k$  is the Boltzmann constant,  $T$  is the absolute temperature,  $\Lambda$  is the thermal de Broglie wavelength,  $\rho_i = N_i/V$  represents

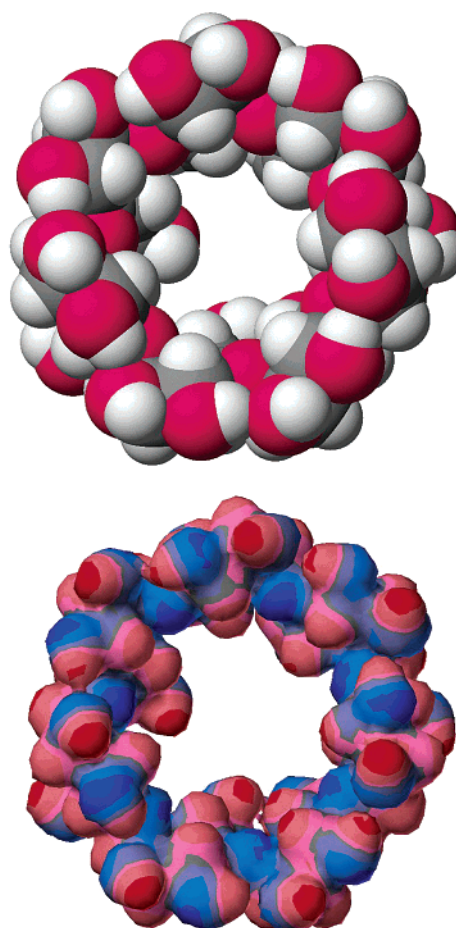


**Figure 2.** Comparison of van der Waals and isodensity surfaces for  $\beta$ -CD. The electron-isodensity surface ( $0.01 \text{ electron}/\text{\AA}^3 \approx 0.0015 \text{ electron}/a_0^3$ ) of the fully AM1-optimized structure is colored according to the electrostatic potential. The color-code changes gradually from blue, which corresponds to the more negative regions, to red, which corresponds to the more positive regions along the surface.

particle density,  $v_i$  is (calculated) molecular volume,  $f$  denotes the fraction of the total volume of the liquid assumed to be available for translation ( $f = 0.023$ ), and  $w_0 = \omega_0 kT_0$  and  $w = \omega kT_0$  ( $T_0 = 298.15 \text{ K}$ ) are the interaction-related constants that form the basis of the model. As an important step toward a unified model, all organic nonassociative liquids included in the model (haloalkanes, aromatics, haloaromatics, esters, and ketones) are assumed to be described by the same interaction-related constants:  $\omega_0 = 5.39$ ,  $\omega = 0.082$ . Within the framework of this unified liquid model, the chemical potential of eq 1 could be used to give good description of a variety of physicochemical properties, including boiling point  $T_b$ , enthalpy of vaporization  $H_{\text{vap}}$ , vapor pressure  $\log \rho^{\text{gas}}$ , Ostwald absorption coefficient  $\log \gamma$ , surface tension  $\sigma$ , and a number of partition and solubility data ( $\log P$ ,  $\log \rho_w$ ) for organic liquids that do not contain associative or strongly polar substituents.<sup>3</sup> In this context, close to 90% of the variance in these properties was accounted for by molecular size as measured by the computed van der Waals molecular volume  $v$ . Van der Waals volumes are good measures of the three-dimensional molecular size, and as illustrated by Figure 2, they also correspond to a good degree to the volume delimited by contours of constant electronic density.

For CD complexation, the general condition of equilibrium applies, that is the chemical potential of the guest molecule “freely” solvated in water has to be the same as that of the guest molecule “bound” to the cyclodextrin host, which, in fact, is also solvated in water. Despite the unusual properties of water,

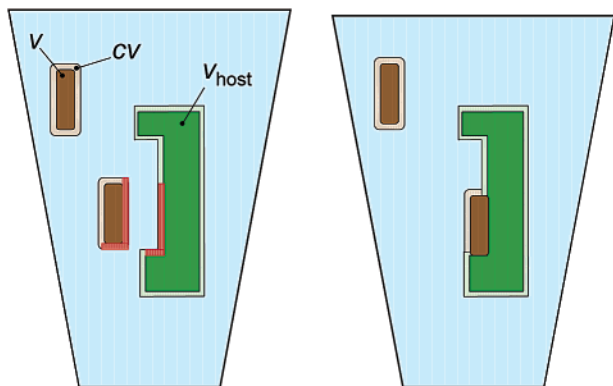


**Figure 3.** Schematic representation of host–guest complexation. Within the present model it is assumed that every solute of molecular volume  $v$  also introduces a “free” volume available for translation (to all molecules in the liquid phase) that is equal to  $cv = fv/(1 - f)$ . During complexation, a volume approximately equal to that of the “free” translational volume associated with the solute becomes inaccessible to the solvent water molecules (denoted in red).

solvation in water can be described by the very same model, but a different, less favorable interaction constant ( $\omega_w = -0.070$ ) has to be used because the unfavorable perturbation of hydrogen bonding in the solvent.<sup>2,3</sup> On the other hand, cyclodextrin-bound molecules can be assumed to be surrounded by the CD environment and experience the usual favorable attractive interaction. Hence, the usual  $\omega = 0.082$  should give a good description of these mostly nonspecific interactions. However, for these molecules, there has to be an unfavorable entropy effect as their movement is much more restricted. They are restricted to only a small fraction of the available volume, as they have to remain CD-bound and cannot just be anywhere within the aqueous phase. Hence, after omitting the  $i$  index denoting the solute, the condition of equilibrium between free  $\rho_f$  and bound  $\rho_b$  solute can be written as

$$kT \ln \left( \frac{\rho_f}{f} \Lambda^3 \right) - \left( w_w + \frac{kT}{v_w} \right) v - w_0 + kT = kT \ln \left( \frac{\rho_b}{f_{CD}} \Lambda^3 \right) - \left( w + \frac{kT}{v_{CD}} \right) v - w_0 + kT \quad (2)$$

For simplicity, we will assume that  $\Lambda$  and even  $w_0$  are identical for both phases. As mentioned, the molecule included in the CD cavity is assumed to be essentially solvated in a CD phase. Therefore, a  $kT(1 - v/v_{CD})$  term is used here as the term resulting from different molecular sizes between solute and solvent and the assumption of volume additivity.<sup>1,3</sup> In the present model, as in that of Hildebrand,<sup>26,27</sup> this term appears as a consequence of the larger increase in the volume of the liquid phase and, hence, the larger increase in the volume available for translation produced by introduction of larger molecules. As long as everything else is identical, solvation in a solute with smaller molecules is more favorable, as a larger number of solvent molecules can access the “free” translational volume that is associated with the solute and is introduced in the solution liquid phase.

The considerable size difference between water ( $v_w = 14.6 \text{ \AA}^3$ ) and CD (e.g.,  $v_{\beta\text{CD}} = 1135.0 \text{ \AA}^3$ ) results in the effective disappearance of the  $v/v_{CD}$  term on the right-hand side. Because the complexed guest molecule in fact still remains within the overall aqueous phase (together with its host), one may reason that the corresponding term (favoring solvation) should not disappear on the right-hand side. However, as Figure 3 shows,

during complexation, part of the “free” volume associated with the solute, which here is assumed to represent a  $c = f/(1 - f) = 0.0235$  fraction of the “hard core” solute volume, will no longer be accessible to the (water) solvent molecules. Looking at host and guest together, and remembering that most organic molecules are linear or flat (and not truly three-dimensional sphere-like) and complexation probably takes place along as much a common surface as possible, the volume that “disappears” is to a good approximation equal to that associated with  $v$ . Therefore, it is not unreasonable to neglect the  $v/v_j$  term on the right-hand side of eq 2. This is probably even more pronounced for  $\alpha$ - and  $\beta$ -CD, in which complexation involves a relatively small cavity, and less pronounced for  $\gamma$ -CD, in which the cavity is larger and more accessible to water molecules even when a not too large guest is present.

The  $f_{CD}$  term denotes the additional volume restriction for “bound” guest molecules. These molecules can move only in the fraction of the liquid volume associated with the CD molecules, which, for sufficiently dilute CD aqueous solutions, can be considered as  $\rho_{CD}v_{CD}/\rho_w^0v_w$ . Furthermore, since the guests are bound inside the CD cavity, they are further restricted to only a relatively small fraction  $\varphi$  of this volume. All these considerations hold for guest that are small enough to be complexed essentially in their entirety with the corresponding CD hosts. Introducing these assumptions in eq 2, and rearranging the logarithmic terms on one side, we obtain

$$kT \ln \left( \frac{\rho_b \rho_w^0 v_w}{\rho_f \rho_{CD} v_{CD} \varphi} \right) = \left( w - w_w - \frac{kT}{v_w} \right) v \quad (3)$$

The  $\rho_b/\rho_f \rho_{CD}$  term introduced by the above assumption into eq 3 is in fact the equilibrium constant,  $K = [\text{CD}(\text{guest}_{\text{bound}})]/[\text{guest}_{\text{free}}][\text{CD}]$ , for the guest–host complexation process:



When determined experimentally,  $K$  is usually obtained based on a molality ( $m$ , mol solute/kg solvent) or sometimes on a molarity ( $M$ , mol solute/L solvent) scale and by assuming that all activity coefficients are close to unity.<sup>7,28</sup> The  $\rho$ 's are number densities, but they can be easily switched to molar densities (mol/L) (by dividing with  $N_0$ ), and for sufficiently dilute aqueous solutions the molality and molarity scales are essentially identical. These assumptions imply that a  $\rho_w^0$  value of 55.2 mol/L value has to be used for water to ensure correct scaling and a unitless quantity under the logarithm. As we can assume room temperature  $T_0$ , one can divide by  $kT_0$  and introduce the corresponding  $\omega = w/kT_0$  terms. We have, therefore

$$\ln \left( K \rho_w^0 \frac{v_w}{v_{CD} \varphi} \right) = \left( \omega - \omega_w - \frac{1}{v_w} \right) v \quad (4)$$

Introducing all the numeric values (the  $\varphi$  fraction being the only undetermined one), we have

$$\ln K = \ln \varphi + \ln \frac{1135.0}{(14.6)(55.2)} + \left( 0.082 + 0.070 - \frac{1}{14.6} \right) v \quad (5)$$

Because  $\Delta G^\circ = -RT_0 \ln K$ , one can easily convert to standard free energies, by multiplying with  $-RT_0$  ( $= -2.479 \text{ kJ/mol}$ ):

$$\Delta G^\circ (\text{kJ/mol}) = -2.48 \ln \varphi - 0.849 - 0.207v (\text{\AA}^3) \quad (6)$$



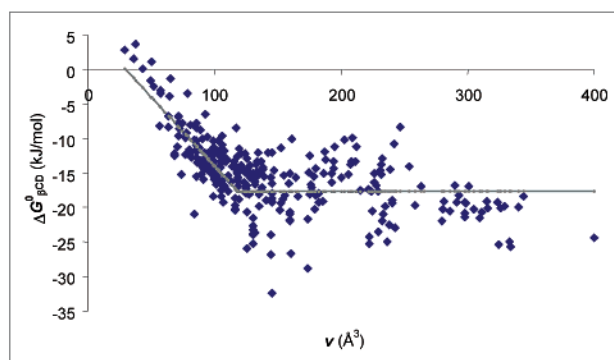


**Figure 4.** Size (molecular volume) dependence of standard free energies of 1:1 complexation with natural  $\beta$ -CD for 310 various guest molecules. The gray line represents the value obtained from the model with an assumed limiting size of  $120 \text{ \AA}^3$  ( $6 - 0.2v$  for  $v < 120 \text{ \AA}^3$  and  $-17.7$  for  $v \geq 120 \text{ \AA}^3$ ).

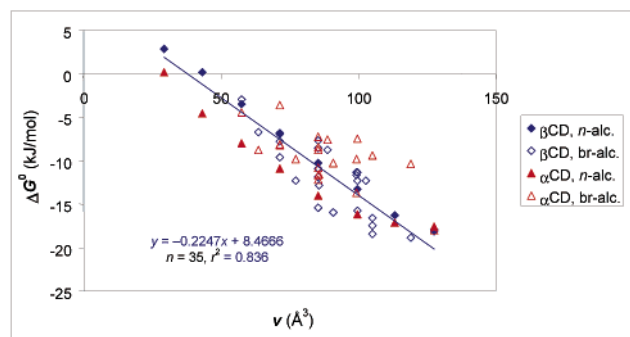


**Figure 5.** Standard free energies of complexation for branched and  $n$ -alcohols (open and filled symbols) with  $\alpha$ - and  $\beta$ -CD (triangles and diamonds), respectively. The trendline represents that of all alcohols combined for complexation with  $\beta$ -CD.

This entirely model-derived slope of  $-0.20$  is in excellent agreement with experimental results. For  $\beta$ -CD, where most data are available, the average slope for all sufficiently small molecules ( $v < 120 \text{ \AA}^3$ ) is  $-0.192$  (Figure 4). For  $n$ -alcohols, which because of their additional flexibility and linearity tend to give a larger slope, the slopes are around  $-0.22$  both for  $\alpha$ - (up to  $n$ -hexanol) and  $\beta$ -CD (Figure 5). This slope gives a general size dependence, but for comparison with another, often used way of presenting size dependence, which works only for congener series, it can be converted to contribution per methylene units. As a methylene ( $\text{CH}_2$ ) unit increases  $v$  almost exactly with  $14 \text{ \AA}^3$ , eq 6 corresponds to a decrease of about  $2.8 \text{ kJ/mol}$  per methylene unit in  $\Delta G^\circ$ , the very same average value suggested by Rekharsky and Inoue in Table 4 of their review.<sup>7</sup>

The value of the intercept is less certain, but a value of around  $5$ – $6$  seems to be a reasonable choice. If a slope of  $-0.2$  is used, best fit (i.e., minimum sum of squared errors) for the basic model assumed here ( $\Delta G^\circ$  decreases linearly for  $v \leq v_{\text{lim}}$  and is constant for  $v > v_{\text{lim}}$ , as shown in Figure 4) is obtained with an intercept of  $6.48$  and a limiting  $v$  of  $121 \text{ \AA}^3$  (corresponding to  $\Delta G^\circ$  of  $-17.7$ ). If the restriction on slope is also relaxed, best fit is obtained with a slightly smaller slope ( $-0.176$ ) and an intercept of  $4.40$  and a limiting  $v$  of  $127 \text{ \AA}^3$  (corresponding to  $\Delta G^\circ$  of  $-17.8$ ). It is reassuring that the value of the slope obtained by fitting to experimental data ( $-0.176$ ) is very close to that obtained from the model ( $-0.207$ , eq 6). On the basis of eq 6, an intercept of  $5$ – $6$  corresponds to a  $\varphi$  value of around  $0.06$ – $0.08$ , indicating that CD-bound guest molecules are restricted to about  $6$ – $8\%$  of the translational space associated with the corresponding CD phase, a very reasonable assumption.

Therefore, with the present model not only the size dependence (slope) of complex stability, but also the corresponding intercept can be obtained on the bases of very reasonable assumptions. It is a remarkable, never before achieved result that the very same  $\omega$  interaction constants derived from boiling point and enthalpy of vaporization data can describe partition, and now complex stability data as well. While it was long obvious that all such intermolecular interaction-related physicochemical properties (e.g.,  $T_b$ ,  $H_{\text{vap}}$ ,  $\log \gamma$ ,  $\log \rho^{\text{gas}}$ ,  $\sigma$ ,  $\log P$ ,  $\log \rho_w$ ,  $\log K_{\text{CD}}$ ) have to be connected, it is for the first time that they could be placed within the framework of a unified and quantitative model at least for nonassociative organic liquids.

Obviously, CD cavities have an upper limit (Figure 1) that is also shape-dependent. Molecular volume gives only an overall size estimate, whereas the quality of the fit certainly has to be shape-dependent. Flexible and rigid guests also behave differently, as flexible guest can more easily adopt a configuration better suited for inclusion. Complex stability data on alcohols (Figure 5) nicely confirm this. Whereas linear and, hence, flexible  $n$ -alcohols give a linear trendline both for  $\alpha$ - (up to  $n$ -hexanol) and  $\beta$ -CDs, the data of branched and cyclic alcohols are much more scattered. For  $\alpha$ -CD, which has a relatively small inside cavity, all branched alcohols give less stable complexes than the linear alcohols of corresponding size (Figure 5). For  $\beta$ -CD, which has a larger inside cavity, branched alcohols give both less and more stable complexes than the linear alcohols of corresponding size (Figure 5). The linear trend of decrease in  $\Delta G^\circ$  for  $n$ -alcohol complexation with  $\alpha$ -CD is maintained about up to  $n$ -hexanol; existence of a limiting size is increasingly apparent for larger guest (Figure 5). Any guest molecule larger than some upper limit for the corresponding CD, will be able to participate in complexation only with some structural subunit.

Experimental complexation data for  $\beta$ -CD (Figure 4), where by far the most data are available ( $n = 310$ ), confirm this general idea. The free energy decreases linearly with size up to about  $120$ – $130 \text{ \AA}^3$ , and more or less levels off after this. The average value for molecules with  $v > 120 \text{ \AA}^3$  is  $-17.7 \text{ kJ/mol}$ . This very simplified model that is represented by the gray line in Figure 4 and that takes into account absolutely no shape- or specific interactions-related effects already accounts for more than  $50\%$  of the variance ( $r^2 = 0.52$  between experimental and “predicted” values, see eq 8). This further confirms that, despite the large functional variety of the more than  $300$  organic molecules with available data, nonspecific interactions are dominant in determining CD-complex stability.

Only about half as much experimental complex-stability data are available for  $\alpha$ -CD ( $n = 179$ ), and they also agree to a good extent with these prediction (Figure 6). The value of the limiting  $v$  is less obvious here, it could be somewhere around  $90$ – $100 \text{ \AA}^3$ . Sufficiently flexible molecules can still give a good fit even for relatively large sizes, whereas rigid molecules might not give a good fit at considerably smaller sizes. The average for molecules larger than  $90$ – $110 \text{ \AA}^3$  is quite stable and is about  $-12.7 \text{ kJ/mol}$ . The slope of the linear section of all data is somewhat less certain than for  $\beta$ -CD, but it seems to have a very similar, maybe slightly more negative value. For  $n$ -alcohols up to hexanol ( $v = 99.5 \text{ \AA}^3$ ), the slope for  $\alpha$ -CD is essentially the same as for  $\beta$ -CD (Figure 5). As Figure 6 shows, the same equation used for  $\beta$ -CD complexation ( $6 - 0.2v$ ) also gives a good fit for the  $\alpha$ -CD data if it is assumed that a limiting value is already reached at a smaller size ( $v = 95 \text{ \AA}^3$ ). However, the overall fit is poorer than it was for  $\beta$ -CD: the model accounts for only about  $25\%$  of the variability here.

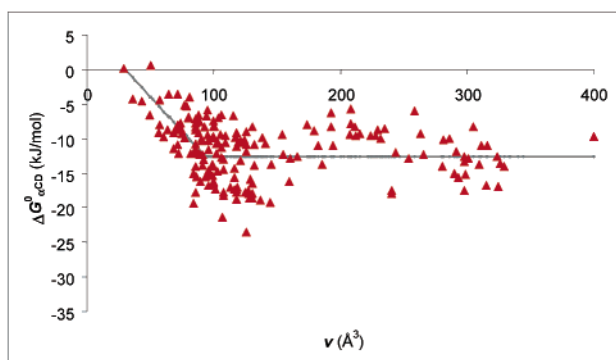


**Figure 6.** Size dependence of standard free energies of 1:1 complexation with natural  $\alpha$ -CD for 179 various guest molecules. The gray line represents the value obtained from the same model as used for  $\beta$ -CD, but with an assumed limiting size of  $95 \text{ \AA}^3$  ( $6 - 0.2v$  for  $v < 95 \text{ \AA}^3$  and  $-12.7$  for  $v \geq 95 \text{ \AA}^3$ ).

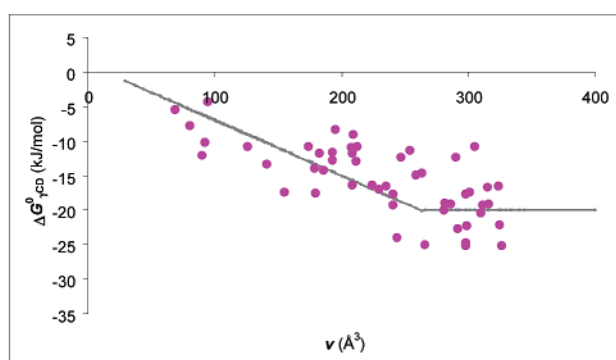


**Figure 7.** Size dependence of standard free energies of 1:1 complexation with natural  $\gamma$ -CD for 51 various guest molecules. The gray line represents the value obtained from the model discussed in the text ( $1 - 0.08v$  for  $v < 260 \text{ \AA}^3$  and  $-20.0$  for  $v \geq 260 \text{ \AA}^3$ ).

Much less ( $n = 51$ ) data are available for  $\gamma$ -CD, and because most published values are for drugs, data is especially lacking on simple structures. Nevertheless, the limiting size seems much larger; it may be around  $250\text{--}300 \text{ \AA}^3$ , but on the bases of available data, it is difficult to pinpoint (Figure 7). It is also obvious that for molecules smaller than this limit, the slope is smaller, probably somewhere around one-third of the value of  $-0.20$  used for  $\beta$ -CD. This can be easily rationalized, because  $\gamma$ -CD has a much larger inside cavity, and contrary to  $\alpha$ - and  $\beta$ -CD, water is not entirely excluded from the cavity during complexation of most molecules. Hence, the guest will not be surrounded entirely by a CD "environment", and the average favorable interaction will be less pronounced here ( $\omega_{\text{avg}} < 0.082$ ). Also, as the fit is much less specific (especially for smaller molecules), the position of  $\gamma$ -CD-bound molecules is much less restricted, and the intercept might be considerably less positive. For example, the eq  $1 - 0.08v$  for  $v < 250$  corresponds to reasonable values of  $\varphi = 0.5$  and  $\omega_{\text{avg}} = 0.03$  and is in good agreement with the experimental data (Figure 7).

The limiting size values obtained here by fitting the model ( $95$ ,  $120$ , and  $260 \text{ \AA}^3$  for  $\alpha$ -,  $\beta$ -, and  $\gamma$ -CD, respectively) certainly represent only approximate values, and actual values also depend on the atomic van der Waals radii used. Nevertheless, they are not unreasonable. For example, the number of water molecules per CD cavity estimated on the bases of crystallization data are  $6$ ,  $11$ , and  $17$  for  $\alpha$ -,  $\beta$ -, and  $\gamma$ -CD, respectively.<sup>29</sup> With the  $v_w$  value used here for water ( $14.6 \text{ \AA}^3$ ), this suggest cavity sizes of around  $88$ ,  $161$ , and  $248 \text{ \AA}^3$  for  $\alpha$ -,

$\beta$ -, and  $\gamma$ -CD, respectively, which are in reasonable agreement with the values obtained here (except of a somewhat larger value for  $\beta$ -CD).

**Complex Stability: Other Effects.** Obviously, size alone cannot account for a considerable amount of variance in the complex stability data, and this is especially true for structures larger than the limiting size requirement of the corresponding CD cavity. Shape or goodness of fit within the cavity is also a major determining factor. For example, the rigid and symmetric adamantyl moiety seems to give an excellent fit within the  $\beta$ -CD cavity and, hence, result in very stable complexes. Di- or trisubstitution of benzene moieties in different positions results in different stabilities, even if size is not affected. There is evidence even for some chiral selectivity.<sup>30</sup> The presence of certain functional moieties (e.g., phenol groups) may also result in specific interactions.

Therefore, we performed a linear regression analysis with the unexplained residual of the present model and a number of structure-derived descriptors. In addition to size and calculated log octanol–water partition coefficient ( $Q\log P$ ), examined variables included the number of rotatable bonds, the number of donor, acceptor, and total hydrogen bonds using a classical additive scale, indicator variables ( $I$ ,  $1$  or  $0$ ) for the presence or absence of a total of more than  $120$  functional moieties (e.g.,  $-\text{OH}$ ,  $\text{Ar}-\text{OH}$ ,  $-\text{NH}_2$ ,  $-\text{NH}-$ ,  $\text{Ar}-\text{SO}_2\text{NH}_2$ , etc.), indicator variables for the presence or absence of structural elements, such as  $-\text{CH}_3$  groups or three- to eight-membered aliphatic, aromatic, or heterocyclic rings.

The model-derived prediction (Figure 4)

$$\Delta G_{\text{model},\beta}^0 = 6 - 0.2v \quad \text{for } v < 120 \text{ \AA}^3$$

$$= -17.7 \quad \text{for } v \geq 120 \text{ \AA}^3 \quad (7)$$

results in

$$\Delta G_{\text{exp},\beta}^0 = 0.440(\pm 0.885) + 1.014(\pm 0.056) \Delta G_{\text{model},\beta}^0$$

$$n = 310; r^2 = 0.515; \sigma = 3.58; F = 327.1 \quad (8)$$

Out of the additional structure-derived descriptors,  $Q\log P$ , was by far the most relevant ( $r^2 = 0.22$  with the residual for  $\beta$ -CD) indicating that overall lipophilicity/hydrophobicity further enhances complex stability.

$$\Delta G_{\text{exp},\beta}^0 = -0.740(\pm 0.757) + 0.702(\pm 0.055) \Delta G_{\text{model},\beta}^0 -$$

$$1.517(\pm 0.137) Q\log P$$

$$n = 310; r^2 = 0.653; \sigma = 3.032; F = 289.1 \quad (9)$$

Even if inclusion of a general lipophilicity/hydrophobicity term seems justifiable and improves the correlation, inclusion of this additional descriptor already worsens the  $F$  statistics. A further warning sign against inclusion of a general lipophilicity term is that, contrary to  $\beta$ CD, inclusion of  $Q\log P$  provides essentially no improvement in the correlation for  $\alpha$ CD. A number of other investigated descriptors have statistically significant coefficients, and their inclusion improves somewhat the descriptive power of the model ( $r^2$ ,  $\sigma$ ), but the  $F$  statistics are further worsened. Therefore, because the main focus of the present work was not as much to obtain accurate prediction of stabilities, but to prove that cyclodextrin complexation can be included within the general framework of the size-based model, these regressions will not be further explored here. Nevertheless, for illustrative purposes one more of the better performing equations, which includes indicator variables for the presence

of  $-\text{CH}<$  groups, eight-membered rings, and phenol functionalities is presented:

$$\Delta G^0_{\text{exp},\beta} = -0.203(\pm 0.679) + 0.670(\pm 0.049) \Delta G^0_{\text{model},\beta} - 1.554(\pm 0.122) \text{QLogP} - 2.545(\pm 0.400) I_{-\text{CH}<} - 6.159(\pm 1.392) I_{\text{Ring8}} - 1.916(\pm 0.400) I_{\text{Ar-OH}} \\ n = 310; r^2 = 0.731; \sigma = 2.686; F = 164.8 \quad (10)$$

This brief exploration only confirms that complexation is mainly determined by nonspecific interactions, which are to a good extent well-accounted for by the size-based liquid model, and to some degree by overall lipophilicity/hydrophobicity and by the presence of specific interactions such as those by a phenol group. The shape of the included (sub)moiety is also relevant as it determines the goodness of fit. In the present work only a limited number of descriptors were explored, and they might not be the most adequate ones. For example, at the present stage, no electronic descriptors were included and no attempts were made to characterize the positioning of the substitution on aromatic rings, etc. Nevertheless, even with these descriptors, the presence of branched carbons and of eight-membered rings seems statistically relevant, for  $\beta$ -CD (however,  $I_{\text{Ring8}}$  is only made statistically relevant by the presence of adamantyl moieties).

**Heat Capacity.** The transfer of nonpolar solutes in water causes a significant change in heat capacity, as the corresponding partial molar heat capacity in water is usually significantly greater than the molar heat capacity of the pure liquid solute. The corresponding excess molar heat capacity, is most certainly related to changes produced in the hydrogen-bonded structure of the aqueous solvent. As it has been shown recently,<sup>2</sup> the present model could also describe such  $\Delta C_p^0$  data by starting from the assumptions of the modified hydration-shell hydrogen-bond model introduced by Muller.<sup>31,32</sup> The excess molar heat capacity is obtained as the difference of the heat capacity contributions (per mole of H-bond) in the hydration shell  $C_{p,\text{hs}}^h$  and bulk water  $C_{p,\text{b}}^h$ , respectively, multiplied by the number of H-bonds (moles) affected by introduction of the solute  $n^h$ :

$$\Delta C_p^0 = n^h(C_{p,\text{hs}}^h - C_{p,\text{b}}^h) \quad (11)$$

The  $C^h$  heat capacity contributions are calculated from the enthalpy of the hydrogen bonds  $\Delta H_b^0$  and the change in the fraction of broken hydrogen bonds  $f_b$ :

$$C_{p,\text{b}}^h = \Delta H_b^0 \frac{df_b}{dT} = (\Delta H_b^0)^2 \frac{f_b(1-f_b)}{RT^2} \quad (12)$$

A similar relationship also holds for the hydration shell. Muller's original assumptions,  $\Delta H_b^0 = 9.80$  kJ/mol and  $\Delta S_b^0 = 21.60$  J/(mol K) for H-bonds in bulk water and  $\Delta H_{\text{hs}}^0 = 10.70$  kJ/mol and  $\Delta S_{\text{hs}}^0 = 27.36$  J/(mol K) for H-bonds in the hydration shell, result in  $\Delta C_p^0 = 8.917n^h$  at room temperature. Within our model, the number of affected H-bonds  $n_h$  was connected to molecular size through the assumption that the same change in water's hydrogen-bonded structure is also responsible for the altered value of the interaction constant of water ( $\Delta\omega = \omega_w - \omega = -0.070 - 0.082 = -0.152$ ). That is, it was assumed that the molar free energy change  $\Delta G^\circ = -N_0\Delta\omega v = -RT_0\Delta\omega v = 0.377v$  (kJ/mol) is entirely due to the disruption of hydrogen bonding, which in the modified hydration-shell hydrogen-bond model is obtained at room temperature as  $\Delta G^h = \Delta H^h - T_0\Delta S^h = 0.6294n^h$  (kJ/mol).<sup>2</sup> This resulted in  $n^h = 0.599v$ .

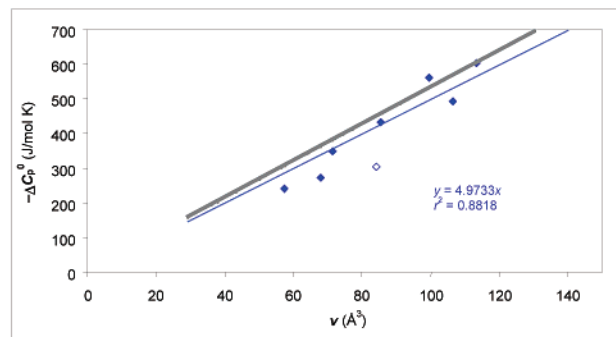


**Figure 8.** Size dependence of the heat capacity of complexation with  $\alpha$ -CD for  $n$ -alcohols, benzene, heptane, and cyclohexane (open symbol). The entirely model-based prediction (gray line) gives an excellent agreement with the experimental data (blue diamonds and trendline).

Hence, the present model suggest the following rough estimate for the size dependence of the excess heat capacity for transfer of nonpolar solutes in water:

$$\Delta C_p^0 \text{ (J mol}^{-1}\text{K}^{-1}) = (8.917)(0.599v) = 5.341v \text{ (Å}^3) \quad (13)$$

For comparison, by using the same conversion as previously, this slope corresponds to an increase in the heat capacity of about 75 J/(mol K) per methylene unit. Available experimental heat capacity data for 1:1 inclusion complexation with  $\alpha$ -CD gives a surprisingly good agreement with this (with an inverted sign as the solute is removed from the aqueous environment) (Figure 8). Data<sup>7</sup> are for  $n$ -alcohols, benzene, heptane, and cyclohexane; cyclohexane is a slight outlier and was omitted from the regression. The trendline with an imposed zero intercept of this experimental data gives a slope of 4.97, in excellent agreement with that predicted by eq 13, 5.341.

The average methylene contribution for the five experimental  $n$ -alcohol data only is 91 J/(mol K). Published heat capacity values of alkylammoniums ( $n = 4$ )<sup>7</sup> are somewhat smaller and also give a somewhat less steep slope, 60 J/(mol K). However, these are charged molecules, and the strong hydration shell associated with the charge may considerably alter the complexation dynamics. The hydration shell will hinder penetration of the entire alkyl chain into the  $\alpha$ -CD cavity. Compared to alkanol guests, amines and acids consistently possess a “disadvantage” of one (or maybe two) methylene units in physicochemical properties that measure the “depth” of CD penetration.<sup>30</sup>

From the experimental alkane and alkene water transport data originally used to obtain the  $\Delta C_p^0$  model,<sup>2</sup> a total of  $n = 5 + 3$  can be used to derive such a per methylene unit size dependence. This gives an average per methylene unit contribution of 70 kJ/(mol K), a value quite similar to that obtained here for ( $\alpha$ )CD complexation. Only very little and much less consistent heat capacity data were available for  $\beta$ -CD complexation, and essentially none was available for  $\gamma$ -CD complexation.

## Conclusions

The complexation thermodynamics of a large number of guests with natural cyclodextrins could be very well-described within the framework of a recently introduced molecular size-based model for nonassociative liquids that also includes a modified hydration-shell hydrogen-bond model for water. With increasing guest size, 1:1 complex stability increases linearly up to a size limit characteristic for each CD, and the corresponding slopes and intercepts for  $\alpha$ - and  $\beta$ -CD are in excellent agreement with those predicted by the model. For larger structures, values level off and are scattered around an average

value depending on shape, goodness of fit, and possibly lipophilicity and some specific effects (e.g., such as those caused by presence of phenol functionality). Limiting cavity size values obtained by fitting to stability data are in reasonable agreement with other estimates, such as those obtained from the number of crystallization water molecules per cavity. Furthermore, for most molecules, heat capacity changes associated with complex formation are also in excellent agreement with those derived from the model based on hydrogen bonding changes in the hydration shell.

**Supporting Information Available:** Table listing data included in the present study. This material is available free of charge via the Internet at <http://pubs.acs.org>.

## References and Notes

- (1) Buchwald, P.; Bodor, N. *J. Phys. Chem. B* **1998**, *102*, 5715.
- (2) Buchwald, P. *Perspect. Drug Discovery Des.* **2000**, *19*, 19.
- (3) Buchwald, P.; Bodor, N. *J. Am. Chem. Soc.* **2000**, *122*, 10671.
- (4) Saenger, W. *Angew. Chem., Int. Ed. Engl.* **1980**, *19*, 344.
- (5) Szejtli, J. *Cyclodextrins and Their Inclusion Complexes*; Akadémiai Kiadó: Budapest, 1982.
- (6) Szejtli, J. *Chem. Rev.* **1998**, *98*, 1743.
- (7) Rekharsky, M. V.; Inoue, Y. *Chem. Rev.* **1998**, *98*, 1875.
- (8) Bodor, N.; Buchwald, P. *Pharmacol. Ther.* **1997**, *76*, 1.
- (9) Bodor, N.; Buchwald, P.; Huang, M.-J. In *Computational Molecular Biology*; Leszczynski, J., Ed.; Elsevier: Amsterdam, 1999; p 569.
- (10) Bodor, N.; Buchwald, P. *Adv. Drug Delivery Rev.* **1999**, *36*, 229.
- (11) Bodor, N.; Buchwald, P. *Med. Res. Rev.* **2000**, *20*, 58.
- (12) Lipkowitz, K. B. *Chem. Rev.* **1998**, *98*, 1829.
- (13) Connors, K. A. *J. Pharm. Sci.* **1995**, *84*, 843.
- (14) Burnette, R. R.; Connors, K. A. *J. Pharm. Sci.* **2000**, *89*, 1389.
- (15) Connors, K. A. *J. Pharm. Sci.* **1996**, *85*, 796.
- (16) Klein, C. T.; Polheim, D.; Viernstein, H.; Wolschann, P. *J. Inclusion Phenom. Macromol. Chem.* **2000**, *36*, 409.
- (17) Klein, C. T.; Polheim, D.; Viernstein, H.; Wolschann, P. *Pharm. Res.* **2000**, *17*, 358.
- (18) Suzuki, T. *J. Chem. Inf. Comput. Sci.* **2001**, *41*, 1266.
- (19) Liu, L.; Guo, Q.-X. *J. Phys. Chem. B* **1999**, *103*, 3461.
- (20) Cai, W.; Xia, B.; Shao, X.; Guo, Q.; Mairget, B.; Pan, Z. *Chem. Phys. Lett.* **2001**, *342*, 387.
- (21) Castronuovo, G.; Elia, V.; Iannone, A.; Niccoli, M.; Velleca, F. *Carbohydr. Res.* **2000**, *325*, 278.
- (22) Hansch, C.; Leo, A.; Hoekman, D. *Exploring QSAR. Hydrophobic, Electronic, and Steric Constants*; American Chemical Society: Washington, DC, 1995; Vol. 2.
- (23) Bodor, N.; Buchwald, P. *J. Phys. Chem. B* **1997**, *101*, 3404.
- (24) Buchwald, P.; Bodor, N. *Curr. Med. Chem.* **1998**, *5*, 353.
- (25) Dewar, M. J. S.; Zoebisch, E. G.; Healy, E. F.; Stewart, J. J. P. *J. Am. Chem. Soc.* **1985**, *107*, 3902.
- (26) Hildebrand, J. H. *J. Chem. Phys.* **1947**, *15*, 225.
- (27) Chan, H. S.; Dill, K. A. *J. Chem. Phys.* **1994**, *101*, 7007.
- (28) Ross, P. D.; Rekharsky, M. V. *Biophys. J.* **1996**, *71*, 2144.
- (29) Brewster, M. E.; Loftsson, T. *Pharmazie* **2002**, *57*, 94.
- (30) Rekharsky, M.; Inoue, Y. *J. Am. Chem. Soc.* **2000**, *122*, 4418.
- (31) Muller, N. *J. Solution Chem.* **1988**, *17*, 661.
- (32) Muller, N. *Acc. Chem. Res.* **1990**, *23*, 23.